The influence of entrance constriction on hydrodynamics and intertidal morphology within estuarine basins

Peter J. de Ruiter[1], Julia C. Mullarney[1], Karin R. Bryan[1], Christian Winter[2]
[1] Coastal Marine Group, Faculty of Science and Engineering, University of Waikato, Hamilton, New Zealand; pd31@students.waikato.ac.nz
[2] MARUM – Centre for Marine Environmental Sciences, University of Bremen, Bremen, Germany

Abstract
We investigate the influence of basin entrance constriction on current velocities, tidal asymmetry, bed shear stresses and intertidal morphology by using a numerical model developed in Delft3D. Hypsometric curves created for six sub-estuaries within Tauranga Harbour indicate a possible link between intertidal hypsometry and entrance constriction. Model results for both spring- and neap tidal cycles show that a constricted sub-estuary with a deep entrance channel is associated with low current velocities and bed shear stresses in the centre of the basin– conditions favourable for sediment deposition. These constricted geometries are shown to be characterized by convex intertidal equilibrium profiles. Unconstricted sub-estuary model results display an even distribution of relatively high current velocities and bed shear stresses resulting in potential for erosion throughout the estuary. The unconstricted basins in our study are mainly associated with concave intertidal equilibrium profiles. Flood dominance increases from the entrance further into the estuary for both constricted and unconstricted conditions.

Keywords: estuaries, sediment transport, hypsometry, tidal asymmetry, Deflt3D

1. Introduction
Terrestrial sediment fluxes to coastal environments can adversely affect ecosystem functioning [17] and may reduce navigability within ports and estuaries [14]. In order to assess the ecosystem state, flow circulations, sedimentary pathways and the connectivity between different regions within estuaries need to be understood.

Intertidal estuarine morphology is controlled by rates of infilling. The local hydrodynamics are responsible for sediment advection and dispersion and generate bottom shear stresses, reshaping the morphology and regulating whether flood currents dominate over ebb currents, creating a non-linear feedback [1], [8]. Observations of intertidal profile shapes are often presented in terms of hypsometry; the total wetted surface area of a tidal flat system as a function of elevation [3]. Intertidal hypsometric profiles become increasingly convex in response to significant accretion, whereas concave profiles tend to occur following erosion [11]. The convex dynamic equilibrium profile is favoured in tidally dominated, flood dominant conditions with sufficient external sediment supply. An increasingly convex profile may favour ebb dominance, initiating seaward sediment transport. Furthermore, when wave energy increases relative to tidal range, intertidal regions experience erosion, becoming progressively more concave [18]. Hence, the orientation of a basin in relation to the fetch can have a significant influence on estuarine morphology [7].

Within large estuarine systems, intertidal regions often exist in smaller sub-estuaries that drain local catchments. These bays vary in size, geometry and orientation and may feature a constricted entrance, often as a result of geological features. The presence of an entrance constriction affects the shape of the tidal wave entering a sub-estuary and therefore influences sediment transport and intertidal morphology. This study focuses on examining the effects of sub-estuary entrance constrictions on current velocities and tidal asymmetry within the bay. We also consider the influence on sediment deposition and erosion potential and the possible link with equilibrium intertidal profile shapes.

2. Study area
Tauranga Harbour, located on the east coast of the North Island of New Zealand (Figure 1) is a barrier-enclosed lagoon covering over 200 km^2. Intertidal flats, exposed at low tide, make up approximately 65% of the harbour [5], with large flats dividing the lagoon into a northern and a southern basin. The harbour has an average water depth of 3 m at low tide [16] and is characterized by a semi-diurnal tide with tidal ranges of 1.62 m at spring tide and 1.24 m at neap tide [6]. The constricted harbour entrances in the north and south may change the amplitude and speed of the tidal wave [15]. The estuary is characterised by a number of sub-estuaries with varying shapes and sizes in both the northern and southern basin, hence it serves as a natural laboratory for studying the physical processes that control the movement and deposition of estuarine sediments [12].

Sediments within Tauranga Harbour are predominantly sandy, with average mud-percentages of 10-30%, similar to other New Zealand estuaries. Increased sediment input,

leading to infilling and turbid waters, is a key stressor of benthic ecologies [17]. Sedimentation rates are elevated in a number of the sub-estuaries such as Te Puna, which was identified as the most depositional as well as one of the muddiest sub-estuaries in the southern basin [2].

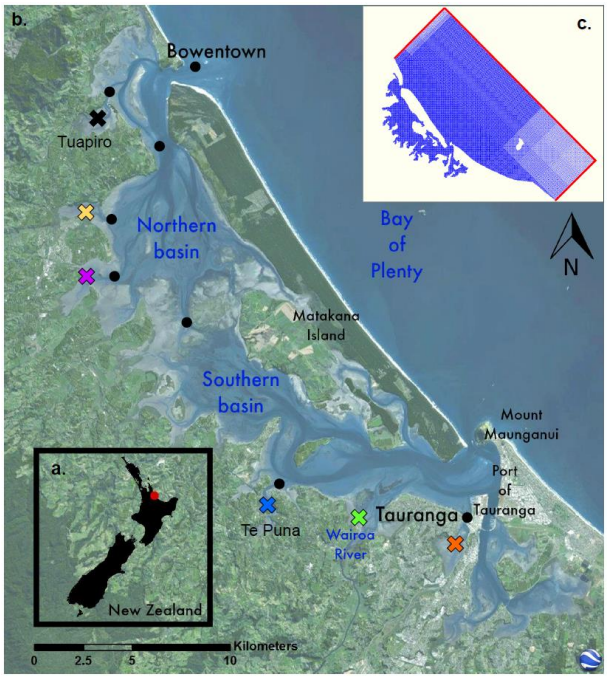

Figure 1 Overview of Tauranga Harbour; location in New Zealand shown by red dot (a). Black dots represent instrument locations (b); coloured crosses depict six sub-estuary locations. The Delft3D model grid is shown (c) with model boundaries in red.

3. Field data

In October 2015, a month-long extensive field campaign was conducted to obtain current velocity and water level data at multiple locations in the northern and southern basin of Tauranga Harbour (Figure 1-b), by deploying current meters and pressure sensors. The data were obtained in both relatively deep areas of the estuary such as the northern harbour mouth and the main estuarine tidal channels, as well as in shallower areas such as tidal flat regions and sub-estuarine channels. Since previous studies of the harbour and current estuary monitoring stations have focused mainly on the southern basin, knowledge of processes in the northern basin is scarce. Consequently, the emphasis of the field deployment was on locations in the northern part of the estuary.

4. Model description

4.1 Modelling system

Numerical simulations were conducted using the Delft3D hydrodynamic modelling system. The model was used to solve the unsteady shallow water equations in a two-dimensional, depth-integrated configuration. A detailed description of these equations and their implementation into Delft3D is given in [9].

4.2 Model setup

4.2.1 Grid and bathymetry

The computational grid used in this study covers both the northern and the southern basin of Tauranga Harbour, as well as an offshore area of roughly 20 by 50 km (Figure 1-c). Inside the estuary, a relatively coarse grid resolution of 100 by 100 m was used in order to reduce computational time. The grid resolution offshore coarsens gradually.

Generation of the model bathymetry was conducted by interpolating high-resolution LiDAR scans from the year 2014 provided by the BoPRC and PoT, complimented by multibeam data and Land Information New Zealand (LINZ) bathymetry data, which were all first converted to Mean Level of the Sea (MLOS) datum. Data coverage was limited for a number of intertidal areas and sub-estuaries.

4.2.2 Forcing

The astronomic tide was forced at the shore-parallel open ocean boundary (Figure 1-c) based on the thirteen largest tidal constituents, derived from the NIWA tidal model [10]. Neumann boundaries were set up for both lateral shore-perpendicular open ocean boundaries. For this study, the effects of wind forcing, waves, and freshwater discharge were not taken into account.

4.3 Model calibration and validation

The model was calibrated and validated against water level and current velocity time series collected during the field campaign. For model calibration a period of 15 days was used, including both spring- and neap tidal cycles, with a simulation time step of 0.1 minutes. Horizontal eddy viscosity and bottom roughness values were varied in order to obtain optimal results. The best calibration was achieved with the Delft3D-FLOW default eddy viscosity value of 10 m^2/s and a spatially varying Manning bottom roughness, between 0.02 and 0.1 $s/m^{-1/3}$, based on variations in bathymetry elevation.

The predictive capabilities of the model were verified by comparing field data and model outcomes for a 12-day period encompassing the second half of the 2015 field campaign. Water levels generally were very well reproduced by the model at all measured locations. The accuracies of modelled current velocities exhibited slightly more variation, with the best results being achieved relatively close to the northern and southern harbour entrances. To assess the quality of the Delft3D-FLOW model predictions, three standard statistical measures of model skill were calculated; the RMSE and MAE to determine model accuracy and the Brier Skill Score (BSS) [13] (Table 1). The

performance rating according to the BSS classification proposed by Sutherland [13] for modelled water levels is 'Excellent' and current speed predictions are classified as 'Good'.

Table 1 Model calibration and validation results. Mean and standard deviations of parameter values for all modelled locations.

Parameter	Water level		Current speed	
	Mean	Std	Mean	Std
RMSE (m)	0.104	0.032	0.135	0.059
MAE (m)	0.082	0.027	0.112	0.056
BSS	0.961	0.024	0.483	0.263

5. Results and discussion

5.1 Hypsometry

Intertidal profile shapes were determined for six sub-estuaries within Tauranga Harbour (locations shown in Figure 1), based on bathymetric data available for these regions. The resulting normalised hypsometric curves (Figure 2) represent the intertidal regions in water depths between the average local entrance channel depth (~1 – 3 m - MLOS) and MHWS (0.86 m + MLOS). For the three bays with a constricted entrance, Tuapiro, Te Puna and Waikareao, hypsometric profiles can be described as convex-shaped. The curves for the remaining bays, Katikati, Tutaekaka and Wairoa whose entrances are unconstricted, display a more concave shape.

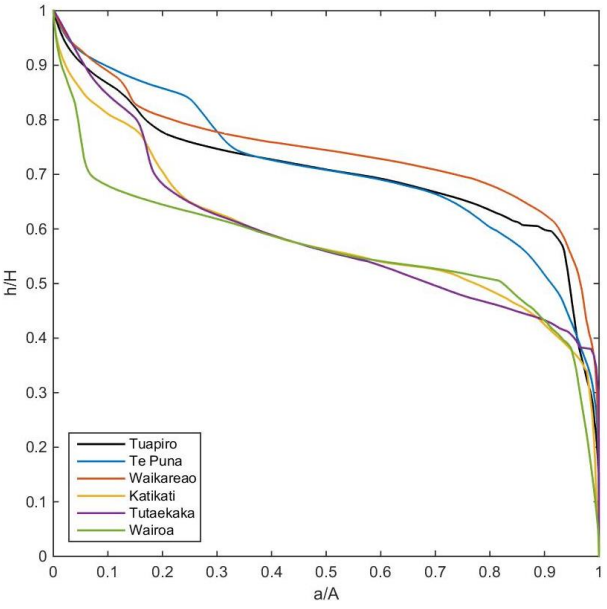

Figure 2 Hypsometric curves for six sub-estuaries within Tauranga Harbour; normalised water depth (*h/H*, where *h* is water depth and *H* is maximum water depth (MHWS)) shown on y-axis, normalised area (*a/A*, where *a* is area and *A* is total subestuary area) on x-axis. Tuapiro, Te Puna and Waikareao, all characterised by a constricted entrance, display a more convex shape than the remaining three unconstricted bays. Line colours match colours of sub-estuary locations in Figure 1.

5.2 Model results

Tuapiro sub-estuary, which features a geometry representative for the constricted bays within Tauranga Harbour, was chosen as a focus region for the modelling study. In order to determine the effects of entrance constriction on current velocities and tidal asymmetry, model runs were implemented for the standard constricted entrance case, as well as for an entrance setting in which the model grid and bathymetry around the entrance were adapted by removing the constriction. Model results were analysed separately for both spring- and neap tidal conditions. Flow velocities and tidal asymmetries were determined throughout the sub-estuary in order to evaluate the effects of entrance constriction on tidal processes in both the main channel as well as the tidal flat regions.

5.2.1 Current velocity patterns

The difference in current velocity characteristics during both flooding- end ebbing tides between a constricted- and unconstricted sub-estuary is shown in Figure 3. A constricted entrance with a small cross section results in relatively high peak depth averaged flood current velocities (~ 0.8 m/s) through the entrance channel (Figure 3-a). The flow cross section increases notably after the narrow entrance channel and there is a great reduction in current velocities, with peak velocities no higher than 0.25 m/s in the centre of the estuary. Similarly, ebb tidal velocities are low in the centre of the estuary, but high ~ 0.6 m/s) through the entrance channel into the main estuary (Figure 3-b). Peak flood velocities are generally higher than peak ebb velocities, indicating a flood-dominant system.

An unconstricted entrance, characterized by a larger cross section, results in lower depth averaged peak flood current velocities (~ 0.55 m/s) through the entrance channel (Figure 3-c). As water enters the central estuary, the flow cross section increases only slightly, resulting in current velocities remaining relatively high (~ 0.4 m/s) compared to the constricted entrance situation. Ebb tides also display a relatively small difference between entrance channel velocities in the entrance channel (< 0.5 m/s) and the central estuary (Figure 3-d). Model results indicate that peak flood- and ebb-current velocities in the centre of the estuary occur slightly earlier in time for an unconstricted basin, both in deeper and shallower areas.

Depth averaged current velocities from the centre of the basin were integrated over transects that include both the channel and the tidal flats, indicated by dotted lines in Figure 3, to produce tidal stage diagrams (Figure 4). Integrations were performed over both a spring- (Figure 4-a) and a neap (Figure 4-b) tidal cycle for both constricted- (blue lines) and unconstricted (red lines) sub-estuaries. In general, the system is flood-dominant

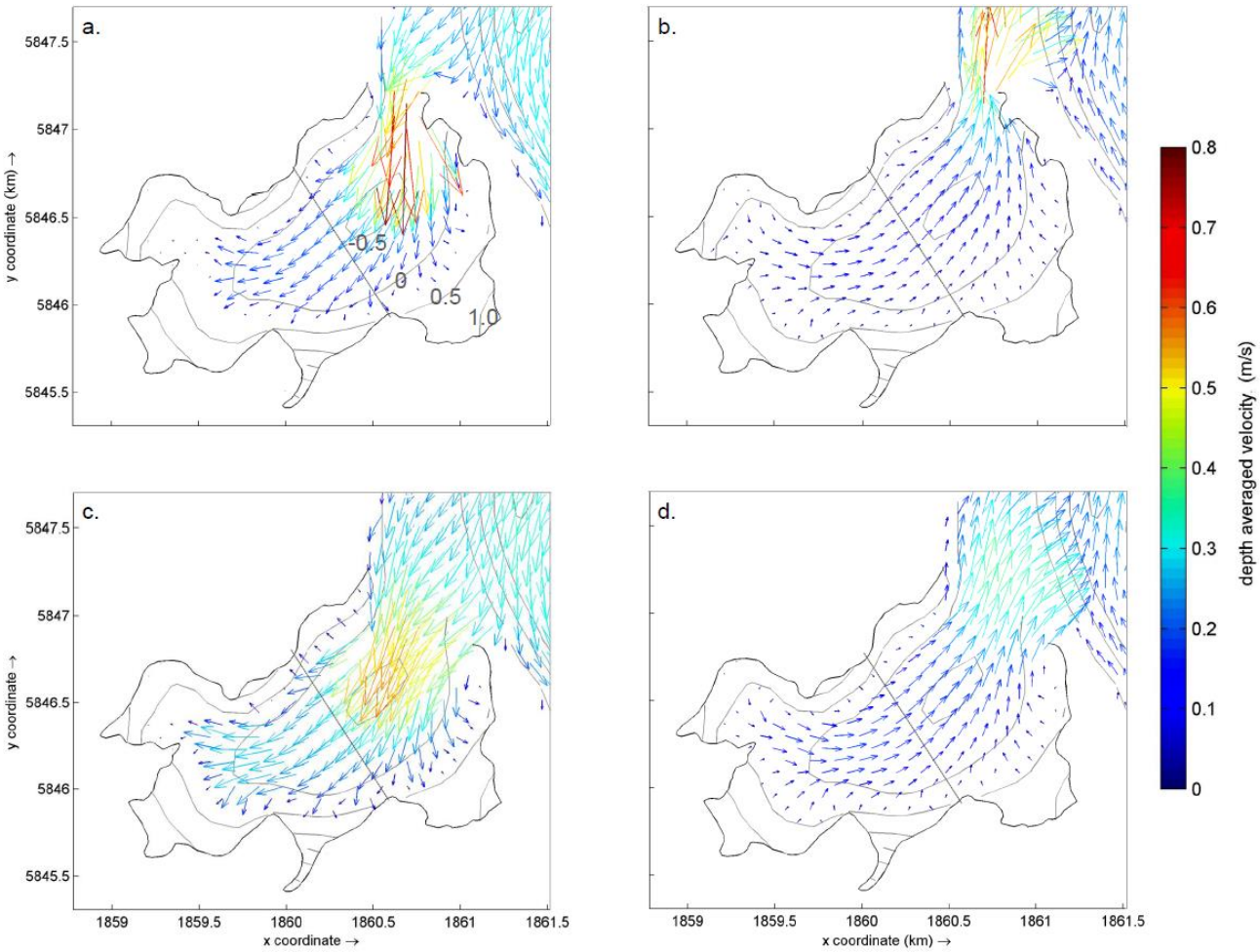

Figure 3 Model results showing depth averaged current velocity patterns in a constricted (a, b) and an unconstricted basin (c, d), for peak flood- (a, c) and ebb velocities (b, d). Dotted lines in the basin centres indicate transects over which current velocities were integrated. Grey lines show depth contours at 0.5 m intervals (values +MLOS, shown in a).

for both spring- and neap tides. Integrated depth averaged current velocities in the centre of the estuary are highest when the sub-estuary entrance is unconstricted (red lines). Overall current velocity patterns are similar for both spring- and neap tidal cycles.

However, there are differences apparent in water levels around high slack tide. During spring tidal conditions (Figure 4-a), water levels at high tide are nearly identical for both the constricted and unconstricted scenario, whereas during neap tidal conditions (Figure 4-b) high slack tide water levels are slightly higher in case of an unconstricted entrance. This water level difference results from the increased volume of water that is able to enter the sub-estuary when the entrance constriction is removed. During neap tides, when water levels rise no further than 0.5 m + MLOS, water is confined mainly within the channels and lower tidal flat areas, thus enhancing the water level difference between constricted and unconstricted cases. During spring tidal conditions, water levels rise to 0.9 m +MLOS, covering a significantly larger area that includes higher tidal flats, reducing any significant water level differences between the two geometries.

5.2.2 Tidal asymmetries

In order to determine changes in rates of tidal distortion throughout the estuary, model results for a number of individual locations were analysed. Amplitudes of M2 and M4 tidal constituents were determined for all locations in order to calculate the sea-surface amplitude ratio M4/M2. This ratio is a direct measure of non-linear distortion [4]. An undistorted tide is characterised by M4/M2 ratios of zero. The results are summarized in Figure 5 for both a constricted and an unconstricted estuary. In both geometries tidal distortion, in this case flood dominance, increases with distance from the estuary entrance. Absolute values of distortion are slightly larger for constricted geometries. At the same distance from the estuary entrance, tidal distortion is larger in the shallower tidal flat areas compared to the estuary main channel. The differences between tidal distortion rates in the channel and on the tidal flats are generally larger for an unconstricted sub-estuary (Figure 5-b). Spring and neap patterns (not shown) were found to be

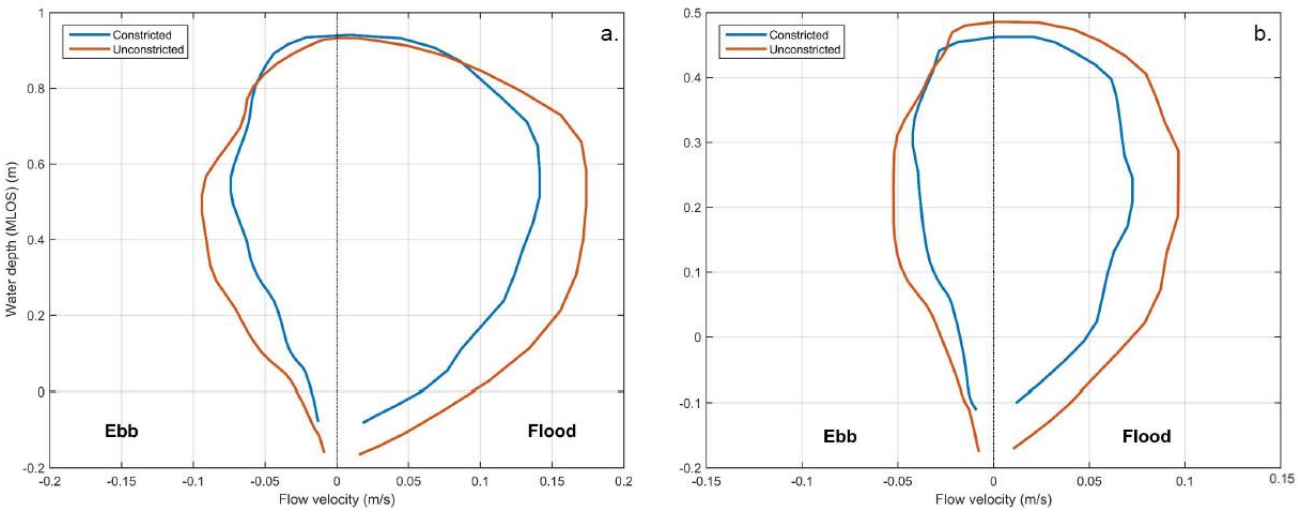

Figure 4 Tidal stage figures showing modelled current velocities versus water depth, integrated over the transect depicted in Figure 3 for spring tide conditions (a) and neap tide conditions (b). Results for constricted entrance situation are shown in blue; unconstricted entrance results in red. Note the change in x-axis and y-axis scale between a and b.

comparable to the general patterns shown in Figure 5 and described above, with tidal distortions being slightly smaller on average during neap tidal conditions. It is worth noting that for an unconstricted sub-estuary during neap tides, tidal distortion rate differences between tidal flats (higher rates) and the main channel (lower rates) are significantly larger than shown in Figure 5. This neap tidal difference in asymmetry may be linked to the water level differences between the unconstricted and the constricted case during neap high slack tide (Figure 4-b), when water levels are mostly limited to the lower portion of the tidal flats.

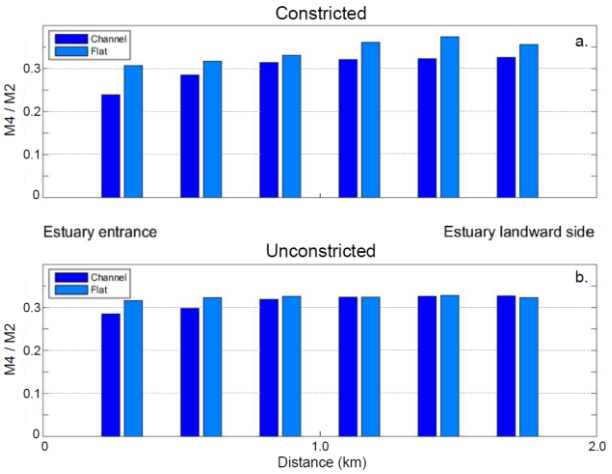

Figure 5 Sea-surface amplitude ratios M4/M2 as a function of distance from the estuary entrance for both the constricted (a) and the unconstricted (b) geometries. Results for the main channel are shown in dark blue; results for tidal flats in light blue.

5.2.3 Bed shear stress

Current velocity patterns and tidal asymmetries influence sediment transport and deposition throughout a basin. Bed shear stress links flow conditions to sediment transport and is therefore an important model output. As implementing the morphology module of Delft3D was beyond the scope of this study, absolute model output values for bed shear stress are not representative of the natural situation and therefore only indicative. However, the shear stress values can still be used to determine in which areas of the estuary erosion or deposition may be expected based on high or low shear stresses, respectively. Figure 6 shows bed shear stresses, corresponding to velocities shown in Figure 3, from zero (no erosion) to high (erosion very likely), for depth averaged peak flood- and ebb current velocities. For a constricted basin (Figure 6-a and Figure 6-b), shear stresses are high in and around the estuary entrance, especially during flooding tide, as a result of high current velocities though the channel. Shear stresses reduce drastically further away from the estuary entrance. This pattern indicates significant potential for erosion in the entrance channel during peak tidal velocities. Further upstream, low bed shear stress indicates a high potential for sediment deposition, especially on the shallow tidal flats. Actual sediment deposition rates are modulated by sediment supply, either from upstream freshwater sources or from the main estuary. When the estuary reaches a relatively stable equilibrium intertidal profile, sediment deposition and erosion rates may become negligible.

In case of an unconstricted basin (Figure 6-c and Figure 6-d), bed shear stresses in and around the entrance are still relatively high, but lower than for the constricted entrance scenario. In the centre of the estuary, shear stresses are reduced, but remain relatively high compared to constricted shear stresses. The higher shear stresses and current velocities throughout the estuary, result in a more

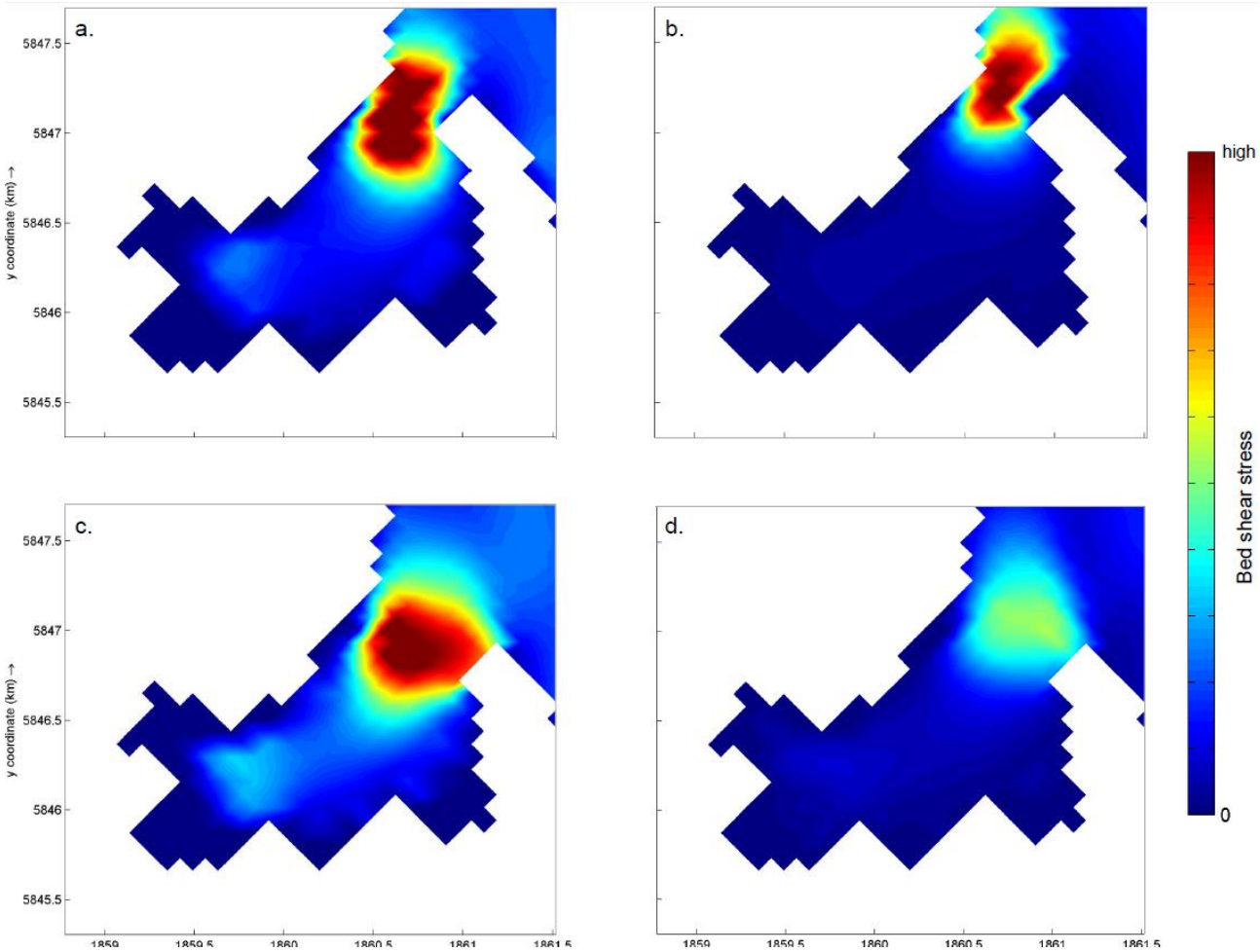

Figure 6 Model results showing indicative bed shear stress patterns in case of a constricted entrance (a, b) and an unconstricted entrance (c, d), for peak flood velocities (a, c) and peak ebb velocities (b, d). Absolute bed shear stress values were not used in this study (see main text for explanation).

evenly distributed potential for erosion. The channel still displays highest erosional potential, but the shallower tidal flats are expected to also experience relatively high erosional rates, with less potential for sediment to deposit in these areas.

5.2.4 Discussion

The entrances of the constricted Tauranga Harbour sub-estuaries are characterized by a relatively deep erosional entrance channel. Low bed shear stresses result in a depositional intertidal environment with high tidal flats corresponding to a convex-shaped hypsometry. The morphologies of these constricted basins may represent a relatively stable equilibrium as a result of dominating tidal processes [3]. Sediment supply modulates the sedimentation rates and corresponding morphological changes in these depositional areas. A sudden increase in sediment supply will most likely result in higher sedimentation rates, resulting in an increasingly convex profile shape and disturbing the equilibrium. As an increasingly convex morphology favours ebb dominance, seaward sediment transport may be enhanced.

The artificial basin with a wide entrance used in the modelling study does not represent an equilibrium unconstricted intertidal geometry, as it is based on the bathymetry of the constricted Tuapiro sub-estuary and the depth of the main tidal channel has not been adjusted. Hence, it is difficult to draw a strong link between hypsometry and unconstricted basins from the model results. In general, the unconstricted Tauranga Harbour sub-estuaries feature a shallower entrance channel than the constricted basins, and may show less potential for sediment deposition on the tidal flats. The result can be a more concave-shaped equilibrium intertidal profile. Highly elevated rates of sediment in discharge fluxes that disturb the dynamic equilibrium, for example as a result of rainfall events, may temporarily increase sediment deposition. Wind and wave effects influence intertidal morphology, especially in case of wide estuary entrances and increased fetch-alignedness [7], and potentially exaggerate concave profile shapes. Differences in rates of infilling between sub-estuaries with varying entrance cross sectional

profiles will be explored in more detail in a follow-up study.

6. Summary

The aim of this study was to examine the relationship between basin entrance constriction, basin hydrodynamics and intertidal morphology. Hypsometric curves of Tauranga Harbour sub-estuaries show that for constricted basins hypsometric profiles can be described as convex-shaped. Unconstricted basins display a more concave intertidal profile shape. Numerical model results concerning current velocities, tidal asymmetries and bed shear stresses were analysed for sub-estuaries with both a constricted and an unconstricted entrance. The flood dominant constricted basin was shown to potentially experience mainly sediment deposition within the centre of the basin and erosion in the entrance channel, resulting in a convex-shaped intertidal morphological profile, as suggested by the hypsometry curves. Results for and unconstricted sub-estuary indicate a potential for erosion throughout the basin, coinciding with a more concave hypsometric curve. Actual sediment deposition rates and equilibrium intertidal profile shapes are modulated by sediment supply, wind and wave effects and geological constraints.

7. Acknowledgements

This research is part of an INTERCOAST (a collaboration between the University of Waikato and the University of Bremen (UB)) PhD study. We wish to thank the Bay of Plenty Regional Council (BoPRC) for funding the research, and Stephen Park from the BoPRC as well as Wade Roest from Port of Tauranga Ltd. for providing Tauranga Harbour bathymetrical data.

8. References

[1] Dronkers, J. (1986), Tidal asymmetry and estuarine morphology. Netherlands Journal of Sea Research, *20*(2), pp. 117-131.

[2] Ellis, J., Manaaki Taha Moana Research, T., Cawthron, I., New Zealand. Ministry of, S., & Innovation. (2013), Ecological survey of Tauranga harbour (Vol. 13). Palmerston North, New Zealand Manaaki Taha Moana Research Team.

[3] Friedrichs, C. T., and Aubrey, D. G. (1996), Uniform bottom shear stress and equilibrium hypsometry of intertidal flats. Washington, DC: American Geophysical Union

[4] Friedrichs, C. T., and Aubrey, D. G. (1988), Non-linear tidal distortion in shallow well-mixed estuaries: a synthesis. Estuarine, Coastal and Shelf Science, 27(5), pp. 521-545.

[5] Healy, T. R., Cole, R., and de Lange, W. (1996), Geomorphology and ecology of New Zealand shallow estuaries and shorelines. New York: John Wiley and Sons.

[6] Heath, R. A. (1985), A review of the physical oceanography of the seas around New Zealand — 1982. New Zealand Journal of Marine and Freshwater Research, 19(1), pp. 79-124.

[7] Hunt, S., Bryan, K. R., and Mullarney, J. C. (2015), The influence of wind and waves on the existence of stable intertidal morphology in meso-tidal estuaries. Geomorphology, 228, pp. 158-174.

[8] Le Hir, P., Roberts, W., Cazaillet, O., Christie, M., Bassoullet, P., and Bacher, C. (2000), Characterization of intertidal flat hydrodynamics. Continental Shelf Research, *20*(12–13), pp. 1433-1459.

[9] Lesser, G. R., Roelvink, J. A., van Kester, J. A. T. M., and Stelling, G. S. (2004), Development and validation of a three-dimensional morphological model. Coastal Engineering, 51(8–9), pp. 883-915.

[10] NIWA. (2015). Tide Forcaster. Retrieved 2015, from http://www.niwa.co.nz/services/online-services/tide-forecaster.

[11] Pritchard, D., Hogg, A. J., and Roberts, W. (2002), Morphological modelling of intertidal mudflats: the role of cross-shore tidal currents. Continental Shelf Research, 22(11-13), pp. 1887-1895.

[12] Spiers, K.C., Healy, T.R., and Winter, C. (2009), Ebb-jet Dynamics and Transient Eddy Formation at Tauranga Harbour: Implications for Entrance Channel Shoaling. Journal of Coastal Research 25(1), pp. 234-247.

[13] Sutherland, J., Peet, A. H., and Soulsby, R. L. (2004), Evaluating the performance of morphological models. Coastal Engineering, 51(8 – 9), pp. 917-939.

[14] Syvitski, J. P. M., Vörösmarty, C.J., Kettner, A. J., and Green, P. (2005), Impact of Humans on the Flux of Terrestrial Sediment to the Global Coastal Ocean. Science 308 (5720), pp. 376-380.

[15] Tay, H. W., Bryan, K. R., de Lange, W. P., and Pilditch, C. A. (2013), The hydrodynamics of the southern basin of Tauranga Harbour. New Zealand Journal of Marine and Freshwater Research 47(2), pp. 249-274.

[16] Tay, H. W., Bryan, K. R., Pilditch, C. A., Park, S., and Hamilton, D. P. (2012), Variations in nutrient concentrations at different time scales in two shallow tidally dominated estuaries. Marine and Freshwater Research 63(2), pp.95-109.

[17] Thrush, S. F., Hewitt, J. E., Cummings, V. J., Ellis, J. I., Hatton, C., Lohrer, A., ... Göteborgs, U. (2004), Muddy Waters: Elevating Sediment Input to Coastal and Estuarine Habitats. Frontiers in Ecology and the Environment, 2(6), pp. 299-306.

[18] Zhou, Z., Coco, G., van der Wegen, M., Gong, Z., Zhang, C., and Townend, I. (2015), Modeling sorting dynamics of cohesive and non-cohesive sediments on intertidal flats under the effect of tides and wind waves. Continental Shelf Research, 104, pp. 76-91.